Progress in Flight Dynamics, Guidance, Navigation, and Control **10** (2018) 199-216
https://doi.org/10.1051/eucass/201810199

ANALYSIS OF GENERIC REENTRY VEHICLE FLIGHT DYNAMICS

Yu. Metsker[1,2], K. Weinand[2], G. Geulen[2], and O. J. Haidn[1]

[1]Technische Universität München, Lehrstuhl für Flugantriebe
München, Germany
[2]MBDA Deutschland GmbH
Germany

The knowledge of reentry vehicles (RV) flight characteristics regarding geometrical shape, dimensions, and mechanical properties is essential for precise prediction of their flight trajectory, impact point, and possible deviations according to simulation uncertainties. The flight characteristic estimations of existing RV require both body dimensions and mechanical properties of the objects. Due to comparatively simple and reliable methods of specifying the vehicle outer dimensions, e. g., photos and videomaterials, the estimation of mechanical properties is a subject of higher uncertainties. Within this study, a generic medium range ballistic missile (MRBM) RV was examined for several modifications such as center of gravity (CoG) position, weight moment of inertia, and initial reentry flight states. Combinations of these variables with constant aerodynamic properties for maximal lateral accelerations will be determined. Basing on these, potential evasion maneuver capabilities of the RV will be described.

ACRONYMS

AoA	Angle of attack
CFD	Computational fluid dynamics
CoG	Center of gravity
DACS	Divert attitude control system
EGM	Earth gravitational model
MSL	Main sea level
MRBM	Medium range ballistic missile
NED	North-East-Down
RV	Reentry vehicle

1 INTRODUCTION

The development of efficient missile defense systems requires as much as possible information about the flight behavior of designated target class at various reentry conditions. This information is used to determine necessary flight characteristics of the interceptor including required lateral acceleration capabilities, closing velocities, and reaction dynamics depending on engagement altitude. Especially, the critical frequency variation of the vehicle during reentry may challenge the attitude control system of the interceptor, intending direct hit. The required maneuver and time constant capabilities should overcome the maximal evasion maneuvers of the RV. Thus, a generic RV was designed to simulate maximal accelerations, critical frequencies, and flight path deviations by variation of mechanical properties and reentry conditions.

The evasive maneuvers of the RV during the reentry can be induced by an active operating divert attitude control system (DACS) or passive measures like CoG displacement or unsymmetrical aerodynamics. Here, DACS devices may be divided into reactive (for example, Post Boost System) and aerodynamically interfering (internal mechanical actuators like reaction wheels or moveable masses, external rudders) classes. Quantifying the maneuverability of a vehicle, two major parameters may be taken into account — maneuver time constant and maximum acceleration perpendicular to flight trajectory. Assuming a DACS to total RV mass ratio of less than 10% for both classes, the maneuverability time constants of conventional technologies can be qualitatively estimated as in Table 1.

The divert maneuverability in aerodynamically interfering systems will be enabled by deflecting the control surfaces or whole vehicle, foregoing by an at-

Table 1 Maneuver time constants for RV with conventional DACS systems

Altitude, atmosphere layer	$\approx$ Vacuum, $h \geq 80$ km	Upper-Tier, $45 \leq h \leq 80$ km	Lower-Tier, $h \leq 45$ km
Attitude maneuverability	None (for aerodynamically interfering systems)	Medium (for aerodynamically interfering systems)	Very small (due to rising dynamic pressure)
	Small (for reactive systems)	Small (for reactive systems)	
Divert maneuverability	None (for aerodynamically interfering systems)	High to medium (for aerodynamically interfering systems)	Small for all DACS systems
	Small (for reactive systems with reasonable operating durations)	Small (for reactive systems with reasonable operating durations)	

titude change with higher dynamics capabilities. Regarding the maneuver time constant for the RV, the Lower-Tier atmosphere layer is most challenging, concerning the required reaction time capabilities of the interceptor, which should be smaller comparing to the target. The maximal lateral deviation capability of the RV utilizing reactive divert systems is limited by the total impulse of the rocket motor and is more reasonable for trajectory correction in upper atmospheric layers to precise the impact point than for divert and attitude control in higher dense atmosphere. Here, aerodynamic forces dominate the maneuverability of the vehicle completely where simulations of passive parameter variations of the vehicle yield the same lateral accelerations on the vehicle as active DACS.

Within the study, several boundary conditions concerning the passive variation parameters will be set. The mass and aerodynamic properties of the RV will be varied within physically reasonable range. As further constrain for the determination of maximal lateral acceleration, a stable flight regime will be defined as such with maximal angles of attack (AoA) of $\alpha \leq 90°$.

2 CASE STUDY

2.1 Reentry Vehicle Parameters

The RV examined in this study presents a typical payload for MRBM. The main characteristic of this class is the use of multiple stages with warhead separation after burnout of the second stage. Figure 1 shows the dimensions of generic nonmaneuvering RV. The example which was chosen for the simulation is a two-staged, solid-propelled missile with total liftoff mass of ca. 21 t. Figure 2 shows

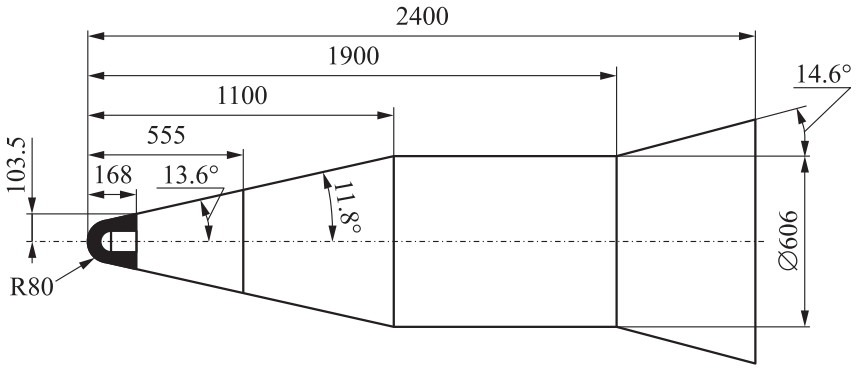

Figure 1 Reentry vehicle dimensions (in millimeters)

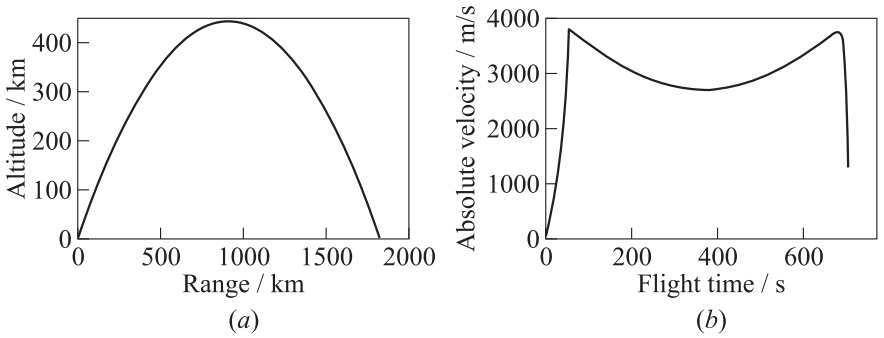

Figure 2 Flight (a) and velocity (b) profiles of two-stage ballistic missile

the flight and velocity profiles of this missile, simulated with an in-house software tool of MBDA GmbH [1].

For a closer investigation, the Lower-Tier atmospheric layer was selected as the most interesting due to low aerodynamic damping effects, resulting in relatively small incidence oscillation frequencies and, consequently, high trajectory deviations.

General parameters of the RV are summarized in Table 2.

Table 2 Main parameters of the RV

Total mass, kg	CoG position (from cone), mm	I_{xx}, kg·m^2	$I_{yy} = I_{zz}$, kg·m^2
740	1303	32.2	224.8

2.2 Simulation Tool

The simulations were performed by "threat analysis and simulation core" — software designed within MBDA GmbH. State of the art Earth gravity EGM96 and climate/atmosphere MSIS-E-90 models for global simulation were used. The software works with a sophisticated boost and thruster model to represent characteristic parameters of several specified rocket engines. The core is capable to simulate multiple objects concerning continuous velocity variation during the ballistic reentry depending on adaptable aerodynamic data quantity and quality. For simulation of RV, full 360° of freedom CFD (computational fluid dynamics) aerodynamic data bases were calculated and implemented. The complete simulation timing is adjustable to fulfill real-time requirements or demands for higher precision of runs. In the current study, the simulations were made with 2-kilohertz frequency.

At reentry velocities over ca. 4000 m/s, ionization effects due to aerodynamic and thermodynamic coupling may occur [2, 3]. This results in boundary layer variation of the RV affecting deviation between real circumstances and CFD simulations. Nevertheless, expected velocities during the reentry of MRBM warheads yield in current simulation ca. 3600–3800 m/s, where ionization effects may be neglected.

2.3 Reference Simulation and Variation Cases

Due to high data workload for a simulation with the complete flight endurance, it is more favorable to analyze only the reentry maneuver with an appropriate variation of initial parameters. For the simulations, a reentry site was selected over the Mediterranean Sea with the initial reference parameters presented in Table 3.

No changes to the reference mechanical settings as mentioned in Table 2 were made. Figure 3 shows the reference reentry trajectory.

Due to trimmed flight parameters, only small oscillations of the aerodynamic AoA occur (see, e. g., Fig. 4). Yaw angle oscillations are located at similar small values.

Due to the absence of roll inducing moments, the acceleration values are not symmetrical to the origin of coordinates and are dominated by Earth gravity

Table 3 Initial reference parameters of the simulation

Inclination angle γ_0	Start altitude h_0, km over MSL	AoA α	Velocity v_0, m/s	Roll rate p_0, deg/s	Velocity azimuth
$-38°$	120	0°	3600	0	90°

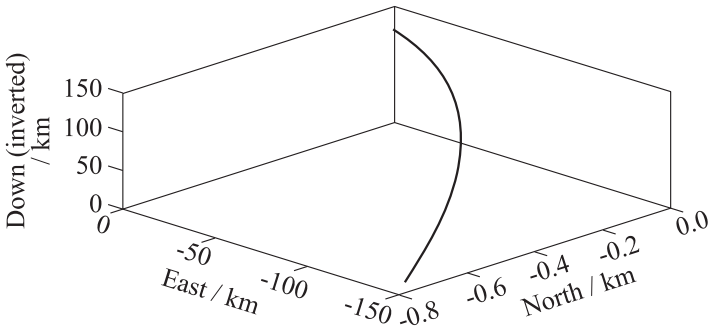

Figure 3 Reference simulation trajectory

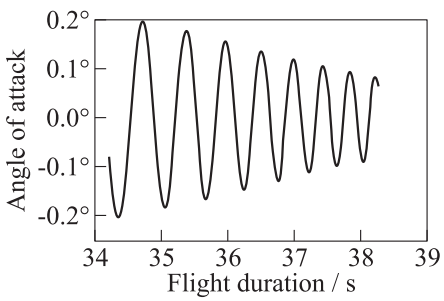

Figure 4 Angle of attack within considered altitude (between 40 and 30 km)

and small aerodynamic drag, resulting from AoA oscillations. Figure 5 shows typical values of acceleration and velocity profiles at altitudes between 40 and 30 km. Lateral acceleration results from external aerodynamic forces taking into account round, rotating Earth.

Integration of the lateral velocities without considering reference frame transformation yields typical deviation history as pictured in Fig. 6.

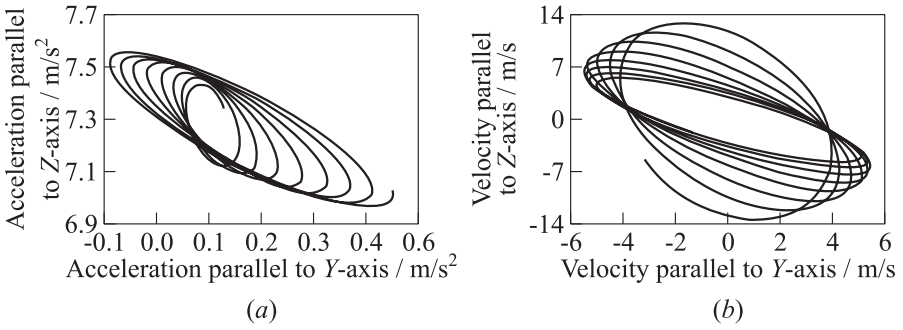

Figure 5 Acceleration (a) and velocity (b) in reference case (body frame), plane normal to undisturbed trajectory, altitude between 40 and 30 km

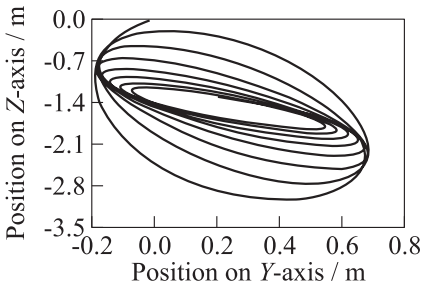

Figure 6 Side location, plane normal to undisturbed trajectory. Position in Body Frame, altitude between 40 and 30 km

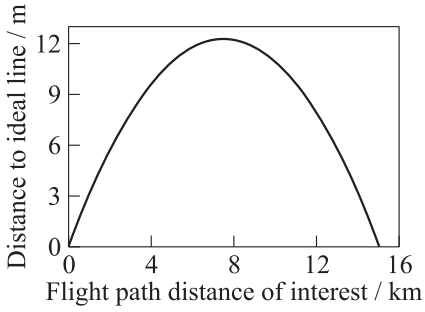

Figure 7 Total displacement of simulated flight trajectory to ideal line

The total displacement of the trajectory may be determined by observing the position in the North-East-Down (NED) frame (Fig. 7). Here, two points on the flight trajectory at the beginning and at the end of a specified altitude are selected and reference line of sight with calculation of normal distances to trajectory points is built. The total deviation is characterized by the curvature of the trajectory influenced rather by Earth gravitation than by aerodynamic effects. Obviously, effects from small aerodynamically induced oscillations and, hence, accelerations shown in Fig. 5*a*, which occur at frequencies of 1.5–2 Hz, have no major impact.

3 ANALYSIS OF PARAMETER MODIFICATION

Reverse engineered RV with well estimated contour still show uncertainties in determination of their real aerodynamic coefficients, total mass, CoG position, moments of inertia as well as possible initial flight condition given by the post boost system. Variation of these parameters will be observed, discussed, and compared to reference simulation case [4].

3.1 Variation of Aerodynamic Coefficients/Derivatives

Aerodynamic coefficient variations may occur by modeling inaccuracies, overseeing small aerodynamic surfaces, assumed area roughness or dimensions. Coefficients with major impact as defined below [5]:

C_A — axial force coefficient;

C_N — normal force coefficient;

C_m — pitching moment coefficient;

C_{lq} — roll damping coefficient due to pitch rate;

C_{mp} — pitch damping coefficient due to roll rate; and

C_{nr} — yaw damping coefficient due to yaw rate

were varied by $\pm 50\%$ with an increment of 2%.

Due to a time-discrete calculation of aerodynamic coefficients within the simulation, these were multiplied each time step by a gain factor. The reference simulation has an amplification factor of 1 in each case (Fig. 8*a*).

A variation of C_A has a very small effect on the range. The range decreases with an increasing C_A by less than 0.5%. This phenomenon may be explained by small residence time of the vehicle within the atmosphere and the chosen

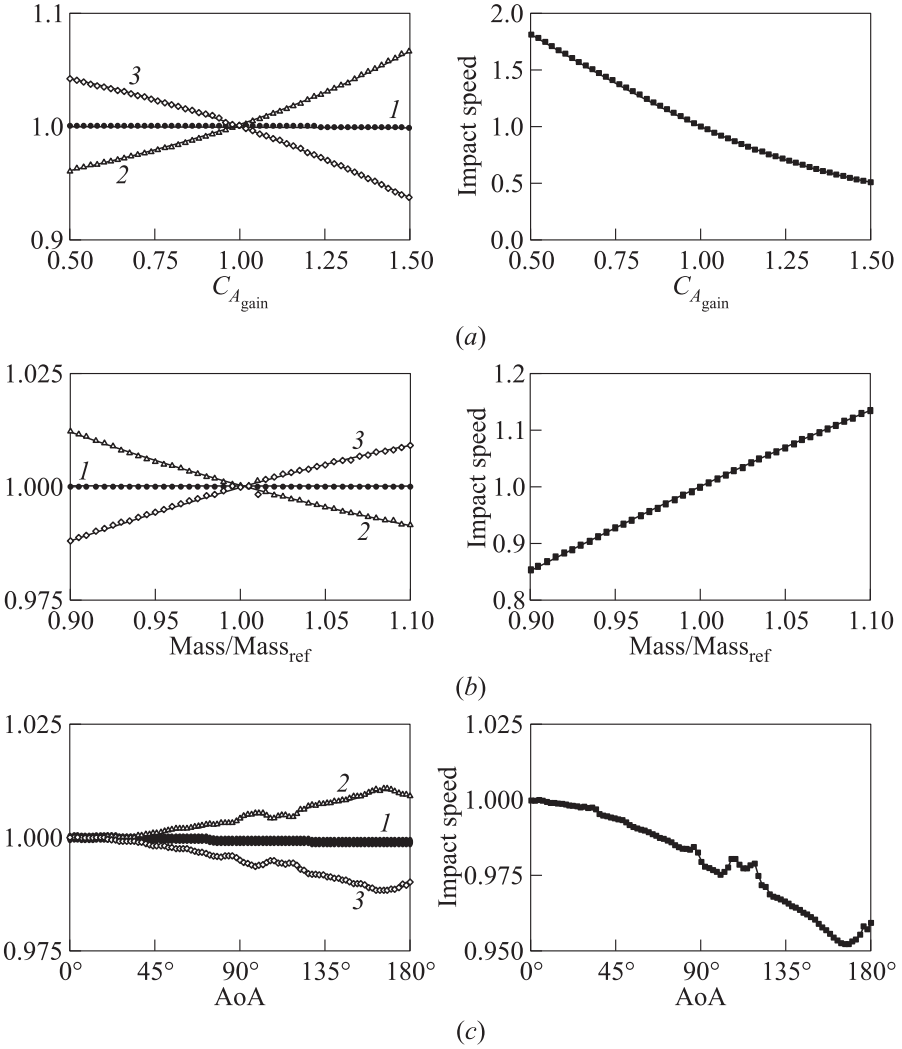

Figure 8 Axial force coefficient (a), mass (b), and AoA (c) variations on range (1), flight time (2), approach speed (3), and impact speed

trajectory inclination, making the horizontal flight range during reentry minimal. In contrast, the flight time increases almost linearly with increasing C_A to a maximum of 107%. Due to the increasing drag by raising C_A, the reentry is decelerated. This is confirmed by the course of the impact speed which decreases from 180% to 50% compared to the reference run over the examined

period. The maximum lateral load factor is unaffected by C_A and is determined by the acceleration due to gravity.

A variation of the C_N and the derivatives C_{lp}, C_{mq}, and C_{nr} has no influence on range, flight time, or approach speed. The maximum load factor in the reentry in the investigated interval results from the gravitational acceleration. An increase of C_N has direct impact on the oscillation of the inclination and leads to their gain, which results in an increasing lateral acceleration. Still maximal deviations from the impact point of the reference simulation yield ca. 9 m.

3.2 Variation of Mass Properties

The variations of the mass are significant for the estimation of expected MRBM range at specified propulsion parameters and reentry deceleration of the vehicle. The mass of the reentry body was varied in the range of $\pm 10\%$ with an increment of 0.5% (Fig. 8*b*).

Higher mass leads to a linear increase of the approaching speed. The range is unaffected by the mass variation. As a result, the speed of approach rises due to falling flight time. The increasing mass in combination with a constant initial speed leads to a greater kinetic energy which is impressed on the reentry at startup. With increasing mass, the ballistic coefficient rises which, in particular, affects the impact speed.

The maximum lateral load factor is virtually unaffected by the mass variation. Due to the aerodynamically undisturbed reentry, the oscillation of the AoA has low magnitude, so that the measured values correspond to the percentage of acceleration due to gravity.

3.3 Variation of Angle of Attack at the Reentry

To investigate the effect of the AoA on reentry behavior, the initial incidence was varied from the reference track from 0 up to 180 degree angle with an increment of 2°. To enable a comparison of the flight paths, the elevation angle was changed in the same direction in order to achieve the same flight path angle for the trajectories (Fig. 8*c*).

With increasing AoA, the flight time increases approximately linearly by about 1%, while the approaching speed decreases to the same extent. A greater influence has to be noted to the impact speed. This is due to the increasing AoA which comes along with increasing aerodynamic drag. This leads to a strong deceleration in deeper atmosphere layers.

With increasing AoA, the maximum lateral load factor rises linearly and reaches a maximum factor of 5.5, compared to the reference case (Fig. 9).

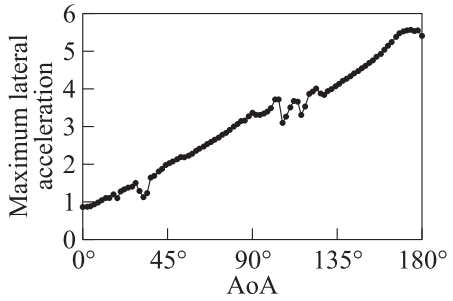

Figure 9 Angle of attack dependence on maximum lateral acceleration

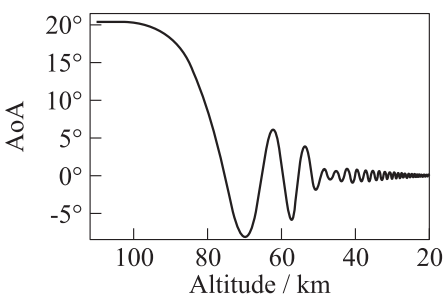

Figure 10 Angle of attack stabilization, altitude between 110 and 20 km

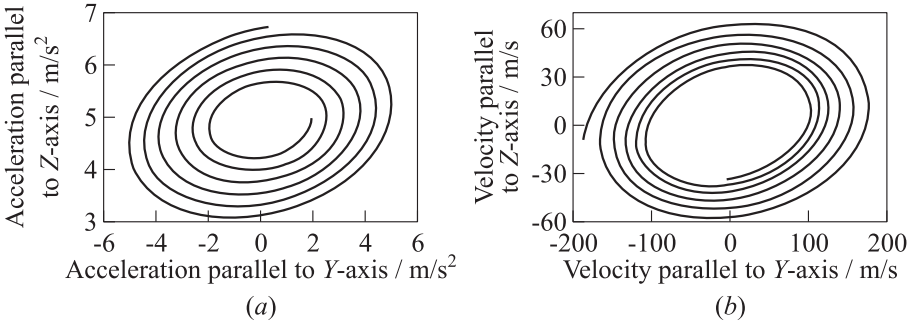

Figure 11 Acceleration (a) and velocity (b) in reference case (body frame), plane normal to undisturbed trajectory, altitude between 40 and 30 km

Stabilization effects dominate the RV movement for initial inclination angle of 20° and default conditions starts at altitudes below 100 km (Fig. 10). The frequencies of the incidence oscillations increase continuously with altitude diminution yielding ca. 2.5 Hz between 40- and 30-kilometer height.

Due to small asymmetry in the aerodynamic coefficients, first coupling effects in pitch and yaw axis occur at altitudes below ca. 60 km. In the reference sector of 40–30 km, lateral accelerations yield amplitudes of 5 m/s^2 and reach maximal values of ± 7 m/s^2 on altitudes between 30 and 20 km.

The observation of lateral accelerations and velocities in the body frame gets imprecise with higher AoA concerning true flight path deviations within kinematic — or NED — frame (Fig. 11). Still, at small incidence angles, total lateral accelerations may be picked as reference criterion for the interceptor missile design. Maximal impact point deviations are also very small, reaching 65 m comparing to the reference case.

3.4 Variation of Roll Rate

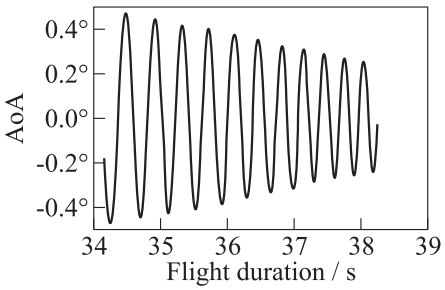

Figure 12 Angle of attack within considered altitude (between 40 and 30 km)

The roll rate was varied in the interval of 0 to 25 rad/s, respectively, 8 Hz, with an increment of 0.5 rad/s. With the examined boundary conditions, there is no effect on the flight performance. Figure 12 shows AoA oscillation during reentry with roll rate of 1 Hz. Here, small coupling effects between the roll frequency and AoA oscillations occur, resulting in slightly higher amplitudes, following by larger lateral accelerations (Fig. 13) compared to the reference case.

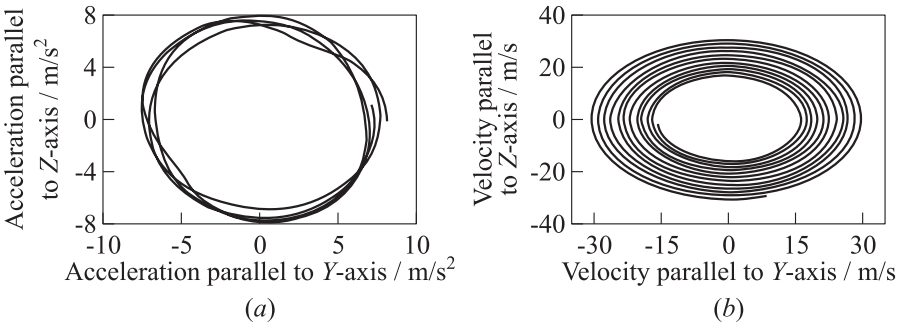

Figure 13 Acceleration (a) and velocity (b) in reference case (body frame), plane normal to undisturbed trajectory, altitude between 40 and 30 km

3.5 Variation of Center of Gravity Offset

Due to typically unknown detailed composition of RV, some assumptions have to be made. Despite desirable geometrical symmetry, deviations in CoG position may be intended to induce pitch and yaw oscillations during the reentry. Thus, offsets in x- and y-directions from the reference case were simulated. Due to Steiner's theorem, CoG offset results in simultaneously adaption of mass moments of inertia.

The CoG of the reentry body in x-direction was varied in the range of $\pm 10\%$ with an increment of 0.5%. Under the examined boundary conditions, only

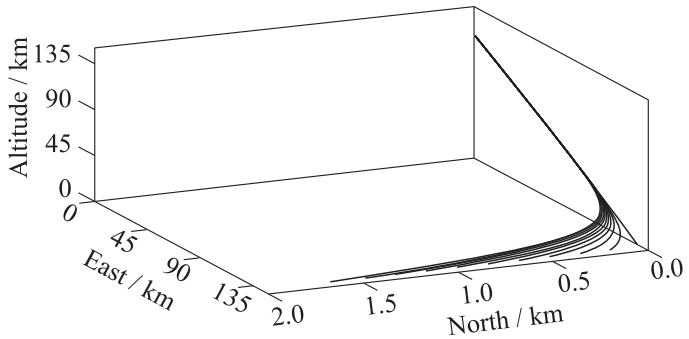

Figure 14 Trajectories of y-CoG offset

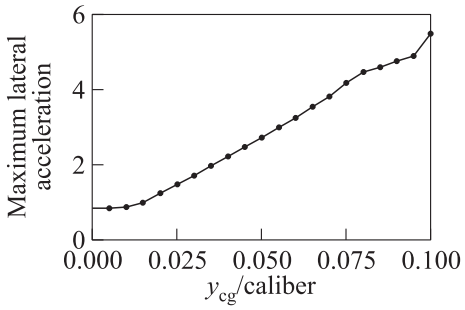

Figure 15 Dependence of y-CoG on maximum lateral acceleration

small effects on flight performance, especially flight time, range, and approaching velocity, were observed (Fig. 14).

Here, an initial displacement of the CoG forward to the cone resulted in higher flight stability and lower energetic losses resulting from smaller AoA oscillations. The CoG displacement backwards to the body end reduces aerodynamic stability and, thus, raises tendency for AoA oscillations. Without coupling of initial parameters like roll rate, AoA incidence, no significant lateral accelerations can be observed. The CoG in y-direction was varied in a range of $\pm 10\%$, based on the caliber, with an increment of 0.5% (Fig. 15).

The impact on the range, flight time, and approach speed is less than 1%. The lever between the aerodynamic center and CoG leads to a yaw movement, whereby a sideslip angle is established. The increased aerodynamic drag results in a reduced impact velocity by up to 5%. Additionally, the increased aerodynamic drag leads to an increasing flying time.

Due to the increasing sideslip angle with higher CoG offset, the maximum lateral acceleration in the reentry increases linearly and rises to a factor of 5.5 compared to the reference case (Fig. 16*a*). The oscillation induction starts below 70-kilometer height and the major effect will be reached at low altitudes, where the air density reaches its maximum (see example in Fig. 16*b*).

The CoG position in z-direction was also varied in a range of $\pm 10\%$ based on the caliber, with an increment of 0.5%. Here, similar effects as with an y-CoG position variation were observed.

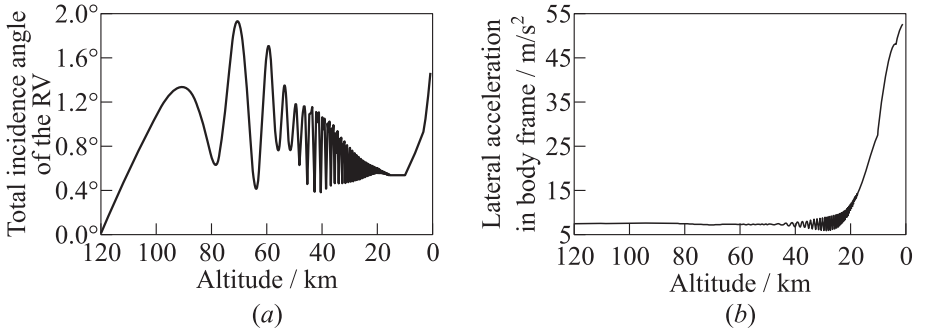

Figure 16 Total incidence angle (a) and total lateral acceleration in body frame (b) at initial y-CoG offset of 0.06 m (10% of the caliber); altitude between 120 and 1 km

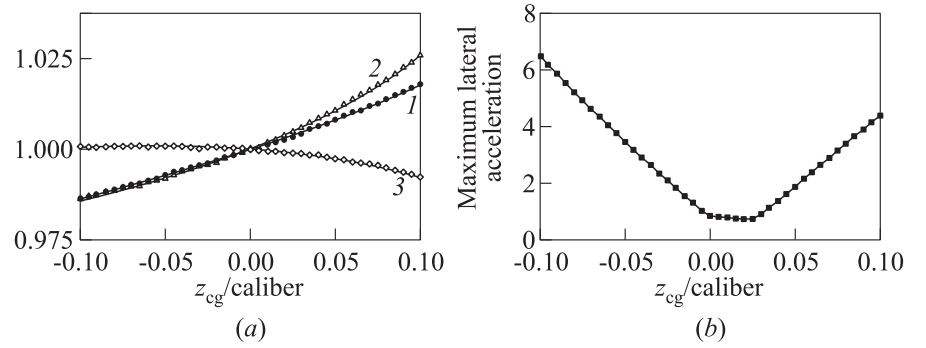

Figure 17 The z-CoG variation on range (*1*), flight time (*2*), approach speed (*3*), and maximum lateral acceleration

The shift in the z-direction leads to a pitching moment due to the lever between CoG and aerodynamic center. A shift in positive z-direction creates a pitching up moment, which leads to an increase of range and flight time of approximately 2% and reduces the impact speed by 14% in comparison to the reference case. According to that, a shift of the CoG in negative z-direction reverses the sign of the resulting moment. This results in a pitching down moment, which decreases range and flight time (Fig. 17a). The impact speed increases by 8% due to the shorter flight phase.

Well-known deviation moments and forces on the RV resulting from y- or z-CoG displacement may be used for the deception of missile defense systems, presuming precise attitude setting of the RV by postboost system and absence of roll-induced moments during reentry. In case of active CoG position control systems combined with inertial navigation and guidance unit, both circular error

probable (CEP) values may be minimized and evasion maneuvers performed. At CoG offsets of 0.06 m, range deviations of approximately 2.5 km in specific case may be achieved, without use of additional aerodynamic surfaces.

3.6 Coupling Between Roll Rate and Angle of Attack

One of the simplest ways to induce lateral acceleration oscillations and hinder interceptor systems during the reentry is to give the RV an initial spin and incidence angle using the postboost system. Simulations with initial incidence angles of up to 40° and roll rates of 25 rad/s, respectively, 4 Hz, were made. A clear tendency of increasing lateral accelerations with higher initial parameter values can be observed (see examples in Fig. 18*a* at values for initial AoA of 10° and roll rate of 1 Hz and in Fig. 18*b* for initial AoA of 40° and roll rate of 4 Hz).

During high frequency and incidence angles conditions, typical oscillation frequencies in the lateral acceleration can be observed. At altitudes between 40 and 30 km, these yield ca. 1.5 Hz and rise up to 6.5 Hz between 20 and 10 km.

The solid curve in Fig. 19 shows the reentry trajectory with a typical helix maneuver of the vehicle at altitudes between 40 and 30 km. The dashed curve represents ideal line between starting point at 40-kilometer and ending point at 30-kilometer height. The deviations from ideal line results from lateral accelerations during the stabilization phase of the vehicle. Calculating normal distances from the trajectory to ideal line yields values given in Fig. 20. While the major curvature with values of up to 15 m can be explained by gravitational and ballistic influence, small peaks result from lateral acceleration oscillations induced by aerodynamic forces.

The displacement resulting from aerodynamically induced forces may be reassessed from the total deviation and is shown in Fig. 21. This altitude range dis-

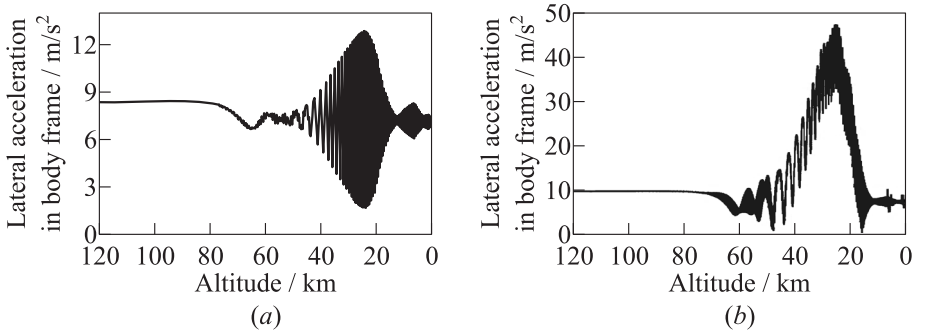

Figure 18 Total acceleration at initial AoA of 10° and roll rate of 1 Hz (*a*) and at initial AoA of 40° and roll rate of 4 Hz (*b*). Altitude between 120 and 1 km

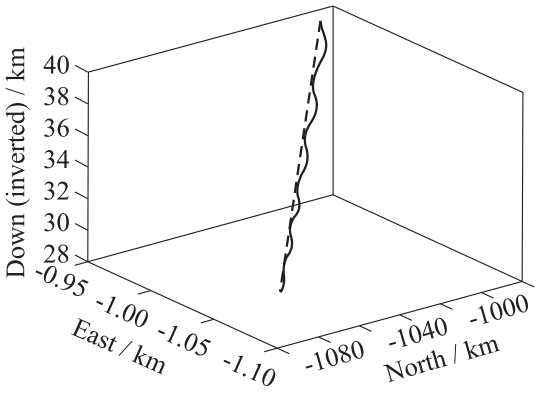

Figure 19 Reentry trajectory in NED frame. Altitude between 40 and 30 km

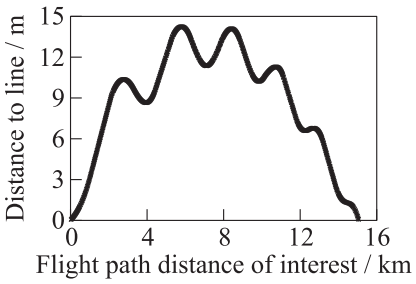

Figure 20 Total displacement of simulated trajectory to ideal line (between 40 and 30 km)

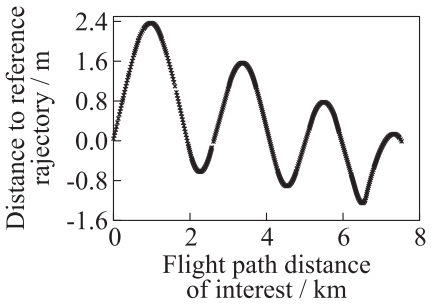

Figure 21 Aerodynamically induced displacement of simulated trajectory (between 35 and 30 km)

plays a distinct frequency peak of 1.5 Hz yielding 2–3-meter deviations from the ideal trajectory (Fig. 22). By exaggerating the oscillation frequencies of 2.5 Hz, the total displacements resulting from lateral accelerations in lower altitudes show the values in the ranges of RV caliber.

The evasion maneuvers of the RV are effective only for deviations exaggerating displacements in magnitude of the RV caliber, which fits for altitudes over ca. 30 km in certain case. By hindering

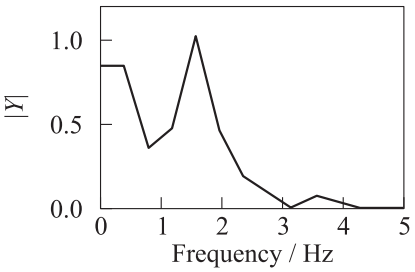

Figure 22 Frequency analysis of displacement history. Altitude between 35 and 30 km

the missile defense with setting of these initial values, a loss of CEP precision has to be taken into account. During simulations with initial incidence angle of 40° and roll rate of 4 Hz, deviations of up to 1 km on impact point were observed.

3.7 Coupling Between *y*-Center of Gravity, Angle of Attack, and Roll Rate

The highest lateral accelerations could be achieved by setting the combinations of high initial y-CoG offsets, moderate incidence angles, and small roll rates. As described in previous subsection, y-CoG offsets induce AoA oscillations at altitudes below ca. 80 km following by high lateral accelerations and stabilization effects below 20 km, where static incidence angles are achieved (see Fig. 16*a*). In case of an initial AoA specification, oscillations occur with higher amplitudes, respectively, accelerations (see example in Fig. 23).

At initial y-CoG offsets of 0.15 m which correlates to 25% of the caliber and incidence angles higher than ca. 16°, the RV is unable to reach stable flight conditions and tumbles at altitudes between ca. 50 and 15 km. Here, AoA reaches the values over 90° where longitudinal axis is positioned perpendicular to kinematic velocity. Total displacements between simulated trajectory and ideal line reach more than 50 m at altitudes between 40 and 30 km leading to high impact point deviations.

Initial roll rate settings stabilize the reentry maneuver and limit maximal lateral accelerations of the RV. Simulations with initial incidence angles of 10°, roll rate of 0.5 Hz, and 0.15-meter y-CoG offset lead to complex lateral acceleration devolutions at high frequencies (Fig. 24). Fast Fourier transformation analyses on the presented acceleration course yield rapid frequency variation without dominating values, resulting in small deviations from ideal trajectory.

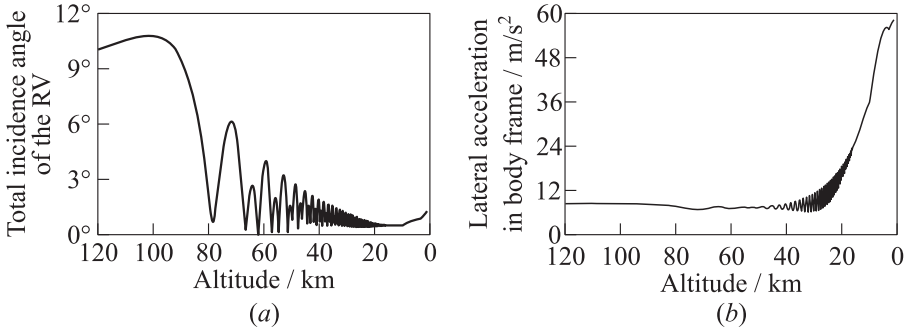

Figure 23 Total incidence angle (*a*) and total lateral acceleration in body frame (*b*) at initial incidence angle of 10° and y-CoG offset of 0.06 m. Altitude between 120 and 1 km

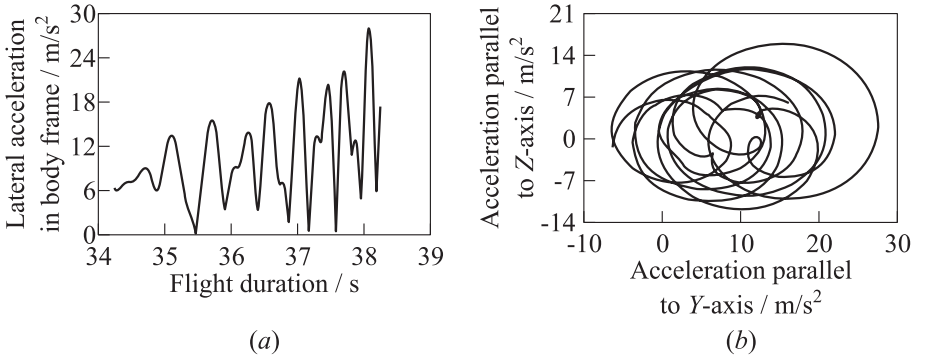

Figure 24 Total acceleration (a) and acceleration in plane normal to undisturbed trajectory (b) with initial incidence angle of 10°, roll rate of 0.5 Hz, and y-CoG offset of 0.15 m. Body frame, altitude between 40 and 30 km

These simulation cases, leading the RV to perform flight dynamic performance just within the stable regime where incidence angles stay below 90°, represent most challenging circumstances for an interceptor, intending the direct hit. Even with small total distance deviations from the ideal trajectory in ranges below 0.5 m, yielding small CEP distances, high frequency oscillations may enhance the seeker noise and thus disturb the interception maneuver. Simultaneously, the approach velocity of the RV decreases raising the reaction time slot of the defense systems.

4 CONCLUDING REMARKS

The variation of flight parameters — roll rate and incidence angle, resulting from the release as well as inherent parameters of the reentry vehicle — CoG position and mass moments of inertia, can be analyzed considering two aspects. The first refers to the impact point of the RV and the second to the lateral flight dynamics, crucial for the development of countermeasure systems.

In comparison to the total flight range, the trajectory deviation resulting from parameter variation may be neglected. Nevertheless, assuming the existence of internal steering devices, the manipulation of CoG position may enhance the precision of intended impact point. Simulations of the RV geometry investigated here showed lateral impact point shift of up to 2 km for CoG displacement of 10%.

Considering lateral flight dynamics, acceleration over 50 m/s^2 was achieved in simulations, coupling inherent and initial flight parameters variation. Manipulations of initial roll rate in combination with incidence angle induce simple

periodical acceleration oscillations where typical frequencies can be observed and their motion evolution predicted by interceptor. Magnitudes of trajectory deviation at frequencies over ca. 2.5 Hz are within the RV caliber, where ideal trajectory assumption for direct hit purposes can be made. Additional modification of inherent parameters yield a complex RV behavior without dominating frequencies in a range of 3–8 Hz making the precise motion and position prediction less reliable. Thus, the interceptor may be able to discriminate the virtual fluctuation center of the RV in the endgame but will struggle on direct hit at suspected, most vulnerable spot of the warhead, considering limited dynamic capabilities.

REFERENCES

1. Weinand, K., and K.-J. Dahlem. 2013. Modellbildung und Simulation für den Fähigkeitserhalt und — aufwuchs der bodengebundenen Luftverteidigung, SGW-Forum der DWT, Modellbildung und Simulation, Bonn.
2. Hirschel, E. H. 2005. *Basics of aerothermodynamics*. Berlin–Heidelberg: Springer-Verlag. 425 p.
3. Ley, W., K. Wittmann, and W. Hallmann. 2011. *Handbuch der Raumfahrttechnik*. München: Carl Hanser Verlag. 846 p.
4. Geulen, G. 2015. Freikonfigurierbare Parameteranalyse einer flugmechanischen Simulation, Masterarbeit, MBDA GmbH, RWTH Aachen.
5. Gallais, P. 2007. *Atmospheric re-entry vehicle mechanics*. Berlin – Heidelberg – New York: Springer-Verlag. 376 p.